Naval Research Laboratory
Washington, DC 20375-5320

AD-A269 755

NRL/MR/5554--93-7389

Morphology and Characteristics of Disturbed HF Skywave Channels

LEONARD S. WAGNER

Transmission Technology Branch
Information Technology Division

DTIC
ELECTE
SEP 2 4 1993
S A D

September 3, 1993

Approved for public release; distribution unlimited.

93-22168

REPORT DOCUMENTATION PAGE

Form Approved
OMB No. 0704-0188

Public reporting burden for this collection of information is estimated to average 1 hour per response, including the time for reviewing instructions, searching existing data sources, gathering and maintaining the data needed, and completing and reviewing the collection of information. Send comments regarding this burden estimate or any other aspect of this collection of information, including suggestions for reducing this burden, to Washington Headquarters Services, Directorate for Information Operations and Reports, 1215 Jefferson Davis Highway, Suite 1204, Arlington, VA 22202-4302, and to the Office of Management and Budget, Paperwork Reduction Project (0704-0188), Washington, DC 20503.

1. AGENCY USE ONLY (*Leave Blank*)	2. REPORT DATE	3. REPORT TYPE AND DATES COVERED
	September 3, 1993	Interim Report (Continuing Program)

4. TITLE AND SUBTITLE

Morphology and Characteristics of Disturbed HF Skywave Channels

5. FUNDING NUMBERS

PE - 61153N33
PR - LR0330244
TA - 033-02-44
WU - 3410-00

6. AUTHOR(S)

Leonard S. Wagner

7. PERFORMING ORGANIZATION NAME(S) AND ADDRESS(ES)

Naval Research Laboratory
Washington, DC 20375-5320

8. PERFORMING ORGANIZATION REPORT NUMBER

NRL/MR/5554--93-7389

9. SPONSORING/MONITORING AGENCY NAME(S) AND ADDRESS(ES)

Office of Naval Research
800 North Quincy Street
Arlington, VA 22217-5660

10. SPONSORING/MONITORING AGENCY REPORT NUMBER

11. SUPPLEMENTARY NOTES

12a. DISTRIBUTION/AVAILABILITY STATEMENT

Approved for public release; distribution unlimited.

12b. DISTRIBUTION CODE

13. ABSTRACT (*Maximum 200 words*)

The normal HF skywave channel is one in which propagation via ionospheric reflection predominates. A disturbed HF skywave channel is defined to be one in which ionospheric scatter plays a significant, often dominant, role in point-to-point radiowave propagation. From a communications perspective, a disturbed channel is one which exhibits reduced signal level in combination with the extensive delay and Doppler spread. Channels which are regularly disturbed include the trans-equatorial, trans-polar and trans-auroral channels. This report covers a number of topics including: (1) measurements that have contributed to our knowledge about the structure and behavior of disturbed channels, (2) solar-terrestrial control factors (e.g., diurnal, seasonal, solar cycle, and geomagnetic), (3) irregularity source regions and current theories of irregularity generation processes, and (4) sample data, available from channel probes, for each of the disturbed channels.

14. SUBJECT TERMS

HF skywave	Pulse sounder
Propagation	Channel characterization
Wideband	Disturbed ionosphere

15. NUMBER OF PAGES

16

16. PRICE CODE

17. SECURITY CLASSIFICATION OF REPORT	18. SECURITY CLASSIFICATION OF THIS PAGE	19. SECURITY CLASSIFICATION OF ABSTRACT	20. LIMITATION OF ABSTRACT
UNCLASSIFIED	UNCLASSIFIED	UNCLASSIFIED	UL

NSN 7540-01-280-5500

Standard Form 298 (Rev. 2-89)
Prescribed by ANSI Std 239-18
298-102

CONTENTS

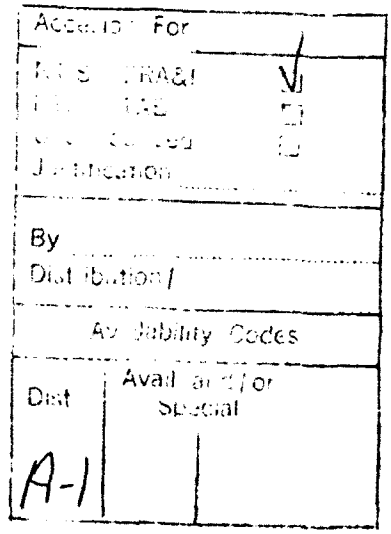

DTIC QUALITY INSPECTED 1

MORPHOLOGY AND CHARACTERISTICS OF DISTURBED HF SKYWAVE CHANNELS

1. INTRODUCTION

For the purposes of this paper, a disturbed HF skywave channel is defined to be one in which ionospheric irregularities play a significant, often dominant, role in determining the characteristics of signals received over the channel. Disturbed channels may vary in degree of disturbance from cases involving weak irregularities embedded in a strong ambient ionosphere, to cases wherein the background electron density may be weak in comparison with that of the embedded irregularity regions. In all cases, the presence of plasma density irregularities tends to degrade communication system performance. Enhanced ionospheric absorption events such as solar X-ray flare events, polar cap absorption events, and auroral substorm absorption events, although frequently associated with disturbed ionospheric conditions, are specifically excluded from consideration in this paper. Such events usually result in "radio blackout" which is characterized by a sudden, catastrophic degradation of channel performance due to signal extinction.

Skywave channels which are regularly disturbed are those involving propagation via the the auroral, polar, and equatorial ionospheres. The winter auroral and polar ionospheres may be classified as ones involving strong irregularity regions embedded in a weak background ionosphere because of the almost complete absence of locally produced photo-ionization at these latitudes. Conversely, because of the extended periods of solar illumination, the auroral and polar regions will be characterized by a strong ambient ionosphere during the summer months. The equatorial region, because of its location, does not suffer comparable fluctuations in solar photo-ionization rates.

The "normal" HF skywave channel is one in which propagation via ionospheric "reflection" predominates. This usually involves negligible frequency dispersion (Doppler spread) and nominal delay dispersion due to the inherent frequency dependent refractive effects of an ionized medium. For disturbed channels, the measured effects will vary with the degree of disturbance. A mildly disturbed channel is usually characterized by weak, large-scale irregularities that introduce tilts in the local ionosphere and associated multipath reflections. These usually entail moderate spreads in delay and Doppler of the order of 100 μs and 1 Hz*, respectively, with variations depending on the specifics of the channel and the path configuration. In the case of strong irregularities, one can expect multipath reflection and scatter from irregularity regions that are spatially distributed about the great circle propagation path (GCP) between the transmitter and the receiver. Delay spreads ranging from 300 μs to 1 ms and Doppler spreads between 5 and 20 Hz may be observed, where the smaller values correspond to signals dominated by multipath reflection returns. Signal strength for a specular-multipath return will be comparable with that observed on an undisturbed channel, while the peak amplitude of a scattered signal will be on the order of 30 dB weaker than that of a reflected return.

In this report I will try to provide a brief summary of the measurements that have been used to characterize the irregularity structure of each of these media. This will be followed, in each case, by a summary of some of the important characteristics related to occurrence statistics, and a brief discussion of the theories used to explain the formation of irregularities. Finally, I will try to summarize what is known of the channel characteristics of each of these media, based on direct measurements of the channel.

2. DISTURBED CHANNELS

2.1 The Equatorial Region

A characteristic of the equatorial region that uniquely affects the dynamical behavior of the equatorial ionosphere is the horizontal orientation of the geomagnetic field lines. Their orientation, perpendicular to the gravitational force, is a key factor in the development of the Rayleigh-Taylor instability at F layer heights, which is a crucial first step in the series of instabilities involved in the development of irregularities.

Manuscript approved June 14, 1993.

* Unless otherwise specified, all values of delay spread and Doppler spread quoted in this paper will refer to the 2σ value as defined by Bello [1965].

Furthermore, F layer irregularities developed in the process will be field aligned, i.e., their dimension along field lines will be much greater than their dimension transverse to the field lines.

Evidence of irregularity structure in the nighttime equatorial ionosphere, in the form of spread F ionograms (equatorial spread F), were first noted by Booker and Wells [1938]. Later evidence in other forms included: (1) coherent VHF backscatter from the equatorial F layer [Farley et al, 1970; Woodman and LaHoz,1976], (2) HF non GCP propagation between Europe and Africa [Rottger, 1973; Rottger, 1976], (3) satellite measurements of equatorial scintillations summarized by Aarons [1978] and by Basu and Basu [1978], and (4) in situ satellite and rocket measurements [Szuszczewicz et al, 1980; Szuszczewicz et al, 1981].

One of the most striking features of equatorial spread F revealed by these measurements is the presence of large depletions of electron density (bubbles) which can extend from the bottomside of the F layer, through the F layer peak, to the topside and which can have a north-south (geomagnetically field aligned) dimension of the order of 1000 km and an east-west dimension of the order of 100 km. Bubbles usually occur in groups that are longitudinally distributed, drift in an easterly direction at speeds between 100 and 200 m/s, and are characterized by sharp gradients of electron density at their edges. In addition to the bubbles, which represent the largest scale sizes in the irregular medium, measurements have also revealed the presence of a spectrum of irregularity sizes extending down to meter scales. The power spectral density of the irregularity spectrum is usually governed by a power law on the irregularity scale size which implies that the spectral intensity decreases exponentially as the scale size decreases. For example, for a power law index of 2, a threefold decrease in scale size results in a 10 dB decrease in the spectral intensity of that Fourier component of the irregularity spectrum. A representative power spectral distribution for the disturbed equatorial F layer (represented in terms of temporal frequency rather than scale size or spatial wave number) can be found in a paper by Szuszczewicz [1986]. A summary of results of experimental measurements up to 1981 can be found in Kelley and McClure [1981].

Equatorial spread F is a nighttime phenomenon with a maximum occurrence frequency between the hours of 1900 and 0300 local meridian time. Late evening ionospheric changes that appear to be connected to the onset of equatorial spread F are: (1) the decay of the bottom-side of the F layer and the associated development of steep, bottomside, vertical gradients of electron density, (2) the rapid vertical ascent of the layer, and (3) the elevated height of the nighttime F layer. Although these conditions usually accompany the development of a nighttime spread F layer, it should be emphasized that their presence does not guarantee its occurrence.

Based on the considerable body of available measurements, of all types, equatorial spread F appears to exhibit a solar cycle, a seasonal, and a longitudinal dependence in addition to its diurnal dependence [Aarons et al, 1980]. The seasonal dependence is manifested in a high rate of occurrence during the equinoctial periods at all longitudes. The longitudinal dependence is manifested in the Atlantic region (encompassing the equatorial regions of South America and West Africa) by a high rate of occurrence during the period November through January and a minimum rate of occurrence during the period May through July. By contrast, the longitudinal dependence in the Pacific region, encompassing longitudes 135-180°E, is the reverse.

The presence of a horizontal magnetic field at the equator, which tends to restrict vertical motions of the ionospheric plasma thereby supporting the plasma against gravitational forces, creates conditions that can lead to a fluid type of instability known as the Rayleigh-Taylor instability. This instability occurs when a heavy fluid is unstably supported atop a lighter fluid. A form of this instability, the collisional Rayleigh-Taylor instability, is generally accepted [Ossakow, 1981; Szuszczewicz, 1986] as the mechanism responsible for the formation of the largest irregularity scale sizes found in the disturbed equatorial F layer, the so-called bubbles. A variety of plasma instabilities [Ossakow, 1981; Szuszczewicz, 1986], driven by plasma drift motions (vertical and horizontal) and by the sharp gradients in the bubble walls, have been proposed and largely validated, as being responsible for the production of field aligned irregularities at all sizes down to meter scale lengths. It is presumed that the aforementioned nighttime events create the conditions conducive to triggering the onset of the Rayleigh-Taylor instability.

Direct measurements of the communications characteristics of the equatorial channel are not extensive. The only available channel probe measurements were made over a 12 day period during July 1986 on a 2158 km east-west path along the geomagnetic equator [Basler et al, 1987]. The midpoint of the path, at a geographic longitude of approximately 162 degrees, and the season, July, were optimally selected for observing spread F effects in the Pacific region. Solar activity, however, was very low, coinciding with a time of solar minimum when the occurrence of spread F is expected to be low.

A scattering function [Bello, 1963; Stein, 1987] representative of these measurements is shown in Fig. 1 in the form of a contour plot. The contours define constant values of signal-to-noise ratio (SNR). The innermost (largest) contour represents a SNR of 25 dB and the contour spacing is 5 dB. The scattering function indicates

a moderate delay spread and a small Doppler spread (at least by the standards of the high latitude disturbed channels which are discussed in the following sections). Delay spreads of the order of 300 to 400 μs, measured at the -10 dB level relative to the signal peak, seem to be typical. Doppler spreads of the order of 2 to 4 Hz are estimated using the same criterion.

For vertically distributed, north-south field-aligned irregularities, and for the given east-west propagation geometry, the Doppler spreading is most sensitive to vertical drift motions which are smaller (30 to 50 m/s) than the west to east drift motion of the region (100 to 200 m/s). It is quite possible that one might observe up to a factor of four increase in Doppler spread, for the same frequency, if one were dealing with a north-south path of comparable length. This is because of the larger east-west drift velocity and because of the greater possibility for oblique path propagation with large lateral offset (e.g. [Rottger, 1973]). Channel probe measurements on a north-south transequatorial path, unfortunately, have not been made.

(U) 2.2 The Polar Region

Irregularity structures in the polar region consist primarily of two kinds, polar arcs and large scale patches [Buchau et al, 1985]. The polar arcs are very long (> 1000 km), thin (~ 100 km) ionization enhancements that are aligned with the earth-sun line. They have been observed using photometric imaging techniques and ionospheric sounders. They occur in association with enhanced fluxes of soft electrons (~ 500 ev) and are most prominent around the time of solar maximum and during magnetically quiet periods. They exhibit no particular diurnal pattern and generally drift across the polar cap from the dusk to the dawn meridian at speeds between 100 and 250 m/s with occasional reversals of drift direction. Their presence leads to scintillation effects on trans-ionospheric propagation paths and spread traces on backscatter ionograms. As yet, there have been no reports of channel parameter measurements when polar arc disturbance conditions have prevailed along the path.

F layer patches are very large regions of enhanced electron density (~ 1000 km in diameter) that are observed to transit the polar region from the noon to the midnight meridian at speeds ~ 1000 m/s. Patches are believed to originate at the noon meridian in the solar illuminated, subauroral region of the daytime ionosphere. Current theory holds that they are dislodged from the subauroral ionosphere as a result of a perturbation in the local interplanetary magnetic field, which temporarily extends the lower boundary of the auroral region equatorward[Anderson et al, 1987]. Once detached, the plasma is swept up by the magnetospherically controlled high latitude convection pattern [Heelis, 1982; Knudsen, 1974; Spiro et al, 1978] and carried across the polar cap in the direction of the midnight meridian. The high electron density gradient at the patch boundary with the ambient polar ionosphere, facilitates a variety of plasma instabilities [Tsunoda, 1988] which are held responsible for the strong irregularity structure associated with these patches.

Patch occurrence rate exhibits a diurnal variation in universal time (UT) which is related to the displacement (~ 10 degrees) of the magnetic pole from the geographic pole. Because the auroral oval and the polar cap are centered on the magnetic pole, and because the orientation of the auroral oval is fixed relative to the earth-sun line, the rotation of the earth causes their positions to undergo a diurnal periodic motion in geographic coordinates. The effect of this motion is that the sub-solar point on the auroral oval (noon , magnetic local time) is at a geographic latitude of approximately 65 degrees at 1700 UT and at a geographic latitude of 82 degrees at 0500 UT. The strong UT modulation of the solar zenith angle at the noontime auroral oval results in a corresponding modulation in the ambient electron density, and an associated increase in the maximum electron density and rate of occurrence of patches transiting the polar region. This UT diurnal effect has been clearly demonstrated in measurements by Buchau et al [1985].

As previously mentioned, polar arcs are not a factor around the time of solar minimum but are an important factor at solar maximum. Patches, on the other hand, are observed during all phases of the solar cycle. Because the maximum electron density of a patch is determined by the electron density of the source region , patches are certain to be more prominent at times of solar maximum. Given the combined effects of polar arcs and patches, a strong correlation between polar irregularity disturbances and the phase of the solar activity cycle is anticipated. Evidence in support of this contention has been provided by Buchau et al [1985].

Because of the extended periods of darkness in the months between November and March, the polar winter ionosphere is dominated by irregularity structures such as patches and polar arcs. This has been well documented by a variety of measurements including satellite in situ measurements of electron density and structure [Singh et al, 1985]. The summer season of almost continuous solar illumination produces a strong ambient ionosphere in which irregularity regions, if there are any, are immersed. Although the published works do not present any data for summertime measurements, Basler [private communication] has indicated that the summertime spread parameters, especially the Doppler spread, are much smaller than those observed at other times of the year.

The diurnal pattern of irregularity occurrence is affected by that of the two structural forms affecting the polar ionosphere. Given the fact that polar arcs are a significant factor during periods around solar maximum, one might expect that any diurnal dependences introduced by patches would be vitiated by diurnally independent effects due to polar arcs. On the other hand, during times around solar minimum, when polar arcs are weak and rare, one would expect a distinct diurnal pattern of irregularity occurrence typical of that of the patches. These diurnal patterns have been confirmed by Buchau et al [1985] using vertical soundings at Thule, Greenland.

The only available channel probe measurements for the polar region are those of Basler et al [1987; 1988]. These measurements were made on a 1913 km path between Narssarssuaq and Thule, Greenland and consisted of three sets of measurements covering the fall, spring, and summer seasons. The measurement period ran from Ocober 1984 through August 1985. This was a period of minimum solar activity implying that patches were the main source of ionospheric irregularities in the polar region.

Examples of channel probe measurements made on October 3, 1984 on a polar channel [Basler et al, 1987] are shown in Fig. 2. These measurements were made at three different times spaced five minutes apart (1928 UT, 1933 UT, and 1938 UT). The ionogram (1931 UT) shows a very diffuse, but recognizable, 1F2 trace with a maximum useable frequency (MUF) of the order of 11.5 MHz. The associated scattering functions are represented by contour plots.with contours of signal-to-noise ratio (SNR). The maximum SNR contour shown on any of the scattering functions is 55 dB and the spacing between contours is 5 dB. All scattering functions show extensive delay and Doppler spread with significant changes in the spread values occurring in a five minute interval.

Average values of Doppler and delay spread for the equinoctial periods were derived by Basler by averaging the March and October data and evaluating the spread values for each 5 minute observation period. These results, from Figs. 50 and 54 in the Basler report [1987], have been adapted to conform, where possible, to what has come to be accepted as a standard form for expressing spread values, i.e. twice the standard deviation of the spread, and here referred to as the 2σ spread. Values for the Doppler and delay spreads, are plotted in Figs. 3 and 4, respectively. The results for Doppler spread show a weak dependence on UT with an average 2σ Doppler spread of ~ 15 Hz at approximately 1400 UT and declining to a value of ~ 12 Hz at approximately 2300 UT. The delay spread is plotted in terms of the mean spread at the -20 dB contour (and at zero Doppler) relative to the spectral peak. The mean delay spread shows a diurnal variation which peaks close to the expected time of maximum effect (~1700 UT). The mean delay spread, averaged over all times of day, is ~ 0.25 ms.

2.3 The Auroral Region

The auroral region has been recognized, for some time, as a region of very strong field aligned irregularities. Early backscatter measurements at VHF [Bowles, 1954; Dyce, 1955] revealed the presence of aspect sensitive scattering from irregularities of electron density in the auroral E layer, thereby confirming the existence of field aligned irregularities [Booker, 1956]. HF backscatter measurements by Bates [1959], established the existence of auroral echoes from field aligned irregularities at F layer heights, as well.

The auroral region is identified by its nighttime visual displays, resulting from the impact of energetic electrons with the neutral constituents of the upper atmosphere. In a more general sense, the auroral region is characterized by the fact that it is the region of the earth's atmosphere that is accessible to the entry of energetic charged particles from the earths outer radiation belt (i.e. Van Allen belt), the magnetosphere, and the interplanetary medium. Furthermore, it is strongly coupled to events in, and exerts an influence upon, the earth's magnetosphere in response to disturbances in the near-earth interplanetary medium and magnetic field. Both of these factors have a profound effect on the occurrence of irregularity disturbances in the auroral ionosphere.

Energetic particle precipitation into the auroral atmosphere is an inherently irregular process both spatially and temporally. Furthermore, the energy spectrum of the entering particles, which is variable, determines the height of deposition of collision initiated ionization. Auroral regions such as the winter or nighttime ionosphere, for which ionization production is wholly dependent upon energetic particle precipitation, are therefore inherently irregular.

Polar patches are an additional source of enhanced ionization in the auroral ionosphere. Patches convect across the polar cap from the noon to the midnight meridian, enter the nightside auroral region at the midnight meridian, and then return to the noon meridian by way of the dawn and dusk sectors of the auroral region. Co-rotation of the neutral atmosphere with the earth results in a complex convection pattern, on the dusk side,

which results in a distortion of the patches into relatively thin elongated regions of irregular electron density which have been given the rather inelegant title of "blobs" [Robinson et al, 1985; Tsunoda, 1988]. These blobs are generally aligned with the equatorward edge of the auroral oval, adjacent to the high latitude boundary of the nightside F layer trough region,. The high latitude boundary of the F layer trough is also a region of strong irregularity development owing to the steep horizontal gradients of electron density that exist there. The combination of the blobs and the F layer trough boundary make this a highly irregular region of the auroral ionosphere.

In addition to the auroral boundary blobs, smaller patches of irregularities, related to isolated regions of particle precipitation, are found within the oval and finally additional blobs are found on the poleward boundary of the auroral oval [Tsunoda, 1988]. All of these factors combine to make the auroral ionosphere a particularly formidable communication medium, especially during the late fall, winter, and early spring seasons.

Measurements [Wagner et al, 1993(a); 1993(b)] indicate that spread conditions on the nighttime transauroral channel do not depend strongly on magnetic conditions. By contrast, spread conditions on the daytime transauroral channel are quite sensitive to disturbed magnetic conditions. Evidence of enhanced daytime spread conditions has been presented [Wagner and Goldstein, 1991; Wagner et al, 1993] for values of $K_p \geq 3$ (K_p is a quasi-logarithmic three-hourly index of magnetic activity with a scale from 0 to 9, with 0 indicating no activity).

Examples of nighttime conditions on a transauroral channel are shown in Figs. 5, 6, and 7. These measurements were made in March 1992, on a 1300 km path between Sondrestrom, Greenland and Keflavik, Iceland shortly after midnight UT. Magnetic conditions were mildly unsettled, $K_p = 2$, and the midpoint of the path lay near the polar boundary of the nighttime oval. An oblique path ionogram depicting ionospheric conditions at the end of the measurement period is shown in Fig. 5 The ionogram shows a complex structure of individual traces, all diffuse, but with strong returns at their leading edges. These suggest a complicated ionospheric spatial environment consisting of a number of strong irregularity regions distributed about the propagation path. Typical slant F scatter behavior, characterized by a monotonically increasing minimum delay with frequency [Bates, 1959], is observed at frequencies above approximately 10 MHz (Fig. 5). This supports the view of a generally irregular ionosphere with embedded field-aligned irregularities.

Two scattering functions, one at a frequency of 7.5 MHz and the other at a frequency of 14.5 MHz, have been selected for examination. The 7.5 MHz frequency was chosen because it lies in a frequency range where individual traces and strong signals are visible on the ionogram. The 14.5 MHz frequency was selected because it lies in the purely slant F scatter region of the ionogram.

A 3-D representation of an unsmoothed scattering function at 7.5 MHz is shown in Fig. 6. The vertical amplitude scale is in units of dB relative to an arbitrary reference. A 10 dB scale marker is indicated on the figure. The average noise level in the scattering function is on the order of 5 dB below the indicated plot floor.

The scattering function of Fig. 6 shows a relatively weak sporadic-E return at a delay of approximately 350 μs on the figure. This is followed by two nearly contiguous returns corresponding to signals from F layer irregularity regions. The peak spectral amplitude, which lies within the part of the scattering function that corresponds to the 1F2 return, is comparable (~94 dB) with that obtained from daytime specularly reflected signals during magnetically quiet times. This suggests that we are dealing with signals which are reflected rather than scattered. The signal differs from daytime reflected signals, however, in that it is extensively spread in both delay and Doppler (2σ values ~200 μs and 6 Hz). Furthermore, the Doppler spread exhibited by many of the stronger individual features in the scattering function is unusually broad, compared with that of a daytime specularly reflected signal. This suggests that the reflecting surfaces have a limited lifetime compared with the duration (~4 s) of the data sample used to calculate the scattering function.

The model proposed to explain these reflected signals is analogous to that of light glinting off of the choppy surface of a swimming pool. It is proposed that a very large, irregular region of elevated electron density will introduce strong horizontal gradients of electron density capable of "reflecting" those radio waves whose frequency is lower than an equivalent MUF established by the electron density distribution within the region and by the given path. Since the medium is irregular and evolving with time, there can be many reflecting "facets" introducing a range of signal delays and Doppler shifts. Finally, since the region is in a constant state of change, individual reflecting facets will have a limited lifetime and will appear to hop around, thereby explaining the spread Doppler characteristic of many of the individual spectral features, and the broad Doppler spread of the overall scattering function. The properties exhibited by the signal at 7.5 MHz would seem to justify its characterization as that of a specular-multipath reflected signal from a time varying region of spatially distributed irregularities.

Two complementary views of the scattering function for 14.5 MHz is shown in Figs. 7(a) and 7(b). Figure 7(a) shows an unsmoothed, 3-D representation of the scattering function similar in form to that of Fig. 6. It illustrates the random quality of the scattering function for a scatter channel. Except for the strongest signals, which appear to have a finite Doppler width, the scattering function appears to be completely uncorrelated in Doppler and in delay. The Doppler widths of the strongest signals resemble those of the spread features observed at 7.5 MHz (Fig. 6) which suggests that they are scattered by irregularity structures having comparable sizes and lifetimes to those responsible for the 7.5 MHz reflected signals .

The contour plot representation of the scattering function of Fig. 7(b) provides a clearer picture of the manner in which energy has been re-distributed on the delay-Doppler plane as a result of passage through the channel. The contours are specified in dB relative to the peak spectral amplitude The peak SNR for this scattering function is ~ 27 dB. The data for the contour plot has been smoothed using 9 and 5 point triangular smoothing windows (in Doppler and delay, respectively).

The peak spectral amplitude of the 14.5 MHz signal in Fig. 7(a) is 62 dB which is ~30 dB below the peak spectral amplitude at 7.5 MHz (Fig. 6). The delay and Doppler spreads of the signal at 14.5 MHz are 750 μs and 15 Hz, respectively, as compared with values of 200 μs and 6 Hz at 7.5 MHz. All of these factors support a hypothesis of a scatter mechanism being responsible for the received signal at 14.5 MHz, as opposed to a specular-multipath reflection mechanism at 7.5 MHz.

3. DISCUSSION

The results presented for the transauroral channel indicate that three types of signals are observed on the channel depending on ionospheric conditions. During magnetically stable daytime conditions, signal characteristics comparable to those of a quiescent midlatitude channel are observed. During disturbed conditions one encounters multipath reflected signals comparable in amplitude to those of the quiet daytime channel but considerably more spread in delay and Doppler. Finally, under disturbed conditions one may also observe scatter type signals which are ~ 30 dB smaller in amplitude than the specular-multipath signals, and somewhat more spread. These results can be concisely expressed in a "Channel Performance Map" which is a scatter plot of measured points plotted on a graph whose ordinate is signal amplitude, in decibels, and whose abscissa is channel spread-factor, where the spread-factor is expressed as the dimensionless product of the measured 2σ delay and Doppler spread values.

An illustration of a Channel Performance Map is given in Fig. 8 for a case involving two experiments conducted by NRL [Wagner et al, 1993(a)] between Sondrestrom Greenland and Keflavik, Iceland. One of the experiments was a daytime measurement at a time of mildly disturbed conditions and the second experiment was a nighttime measurement at a time of relatively quiet magnetic conditions. In spite of the presence of some weak scatter returns, the daytime experiment showed clear evidence of specularly reflected signals at all frequencies probed. The nighttime measurement showed evidence of specular-multipath and scatter returns at frequencies below about 8.5 MHz but only scatter returns at frequencies above 11.5 MHz.

The filled markers on Fig. 8, representing signal points on the Channel Performance Map, are seen to divide up into three distinct groups. The filled black squares represent specularly reflected signals on the daytime channel. They are characterized by large signal levels and negligible spread-factors. Except for those points with amplitudes < 75 dB, the indicated spread-factors are of the order of the measurement resolution. Points whose amplitudes are < 75 dB correspond to a frequency of 7.2 MHz, which was substantially retarded and dispersed in an F1 layer lying beneath the main F2 layer. Their reduced amplitudes and enhanced spread-factors are a consequence of delay dispersion in this underlying layer.

The signal group represented by the reverse video asterisk, represent specular-multipath returns from the nighttime measurement. They are seen to have amplitudes comparable with those of the daytime reflected signals but a spread-factor which is at least two orders of magnitude larger than that of the daytime reflected signals.

The third signal group represents scattered signals both day and nighttime. They are seen to exhibit the largest spread factor of any signal group and to be on the order of 30 dB weaker than either of the reflected signal types.

Finally, the unfilled markers represent measured noise values on the channel. They are included to provide some sense of the signal-to-noise ratio prevailing during the measurements. Each noise point is assigned the

spread factor and marker type (unfilled) of the corresponding signal. This is done for purposes of identification but is otherwise of no significance.

4. SUMMARY AND CONCLUSIONS

Available evidence for the transauroral and polar channels indicate that they are characterized by roughly comparable values of delay and Doppler spread (2σ delay and Doppler spreads of approximately 0.5 ms and 10 to 15 Hz, respectively). A limited set of measurements for the equatorial channel (east-west measurement path) indicated delay spreads comparable to those of the high latitude channels but a signi: antly narrower Doppler spread (~ 4 Hz).

Measurements on the transauroral path indicate that three types of signals are supported by the medium depending on channel conditions and signal frequency. These consist of specular reflected signals of the type that are received from a smooth laminar ionosphere, specular-multipath signals that are randomly distributed in delay and Doppler and have limited lifetimes, and scatter signals. It is quite likely that one should encounter similar classes of returns on the polar and equatorial channels but the data have apparently not been examined for this property.

Finally, it should be mentioned that the available data set for the disturbed channels is far from exhaustive, and what data there is has not been completely analyzed. Additional measurements that would be desirable include summertime polar and transauroral measurements, high sunspot number polar measurements, and trans-equatorial measurements on a north-south path.

5. REFERENCES

Aarons,J., Equatorial scintillations: a review, IEEE Trans. Antennas and Prop., AP25(5), 1977.

Aarons,J., J.P. Mullen, J.P. Koster, R.F. DaSilva, J.R. Medeiros, R.T. Medeiros, A. Bushby, J. Pantoja, J. Lanat, and M.R. Paulson, Seasonal and geomagnetic control of equatorial scintillations in two longitudinal sectors, J. Atmos. and Terr. Phys., 42, 861-866, 1980.

Anderson, D. N., J. Buchau, R.A. Heelis, Origin of density enhancements in the winter polar cap ionosphere, 1987 Ionospheric Effects Symposium Conf. Record, 649-657, 1987.

Basler, R. P., P. B. Bentley, G.H. Price, R. T. Tsunoda, and T. L. Wong, Ionospheric distortion of HF signals, DNA-TR-87-247, 1987.

Basler, R.P., G.H. Price, R.T. Tsunoda, and T.L. Wong, Ionospheric distortion of HF signals, Radio Sci., 23(4), 569-579, 1988.

Basu ,S. and S. Basu, Equatorial scintillations - a review, J. Atmos. and Terr. Phys., 43(5/6), 473-489, 1981.

Bates, H.F., The height of F layer irregularities in the arctic ionosphere, J. Geophys. Res., 64(9), 1257-1265, 1959.

Bello, P.A., Characterization of randomly time variant linear channels, IEEE Trans. on Communication Systems, CS-11(4), 360-393, 1963.

Bello, P.A., Some techniques for the instantaneous real-time measurement of multipath and Doppler spread, IEEE Trans.on Communications Technology, 13 (3), 1965.

Booker, H.G. and H.W. Wells, Scattering of radio waves by the F-region of the ionosphere, Terr. Magn. Atmos. Elect., 43, 249, 1938.

Booker, H.G., A theory of scattering by nonisotropic irregularities, J. Atmos. Terr. Phys., 8, 204-221, 1956.

Bowles, K.L., Doppler shifted radio echoes from aurora, J. Geophys. Res., 59, 553-555,1954.

Buchau, J , E.J. Weber, H.C. Carlson, J.G. Moore, B.W. Reinisch, R.C. Livingston, Ionospheric structures in the polar cap and their relation to satellite scintillation, Radio Sci., 20(3), 325-338,1985.

Dyce, R. B., Auroral observed echoes observed north of the auroral zone on 51.9 Mc/sec, J. Geophys. Res., 60(3), 317-323, 1955.

Farley , D.T., B.B. Balsley, R.F. Woodman, and J.P. McClure, Equatorial spread F: Implicationsof VHF radar observations, J. Geophys. Res.,75, 7199, 1970.

Heelis, R. A., The polar ionosphere, Revs. of Geophys. and Space Phys., 20(3), 567-576, 1982.

Kelley ,E. P. and J.P. McClure, Equatorial spread-F: A review of recent experimental results, J. Atmos. Terr. Phys., 43, 427, 1981.

Knudsen, W.C., Magnetospheric convection and the high-latitude F2 ionosphere, J. Geophys. Res., 79 (7), 1046-1055, 1974.

Ossakow, S. L., Spread-F theories - A review, J. Atmos. Terr. Phys., 43, 437, 1981.

Robinson, R.M. R.T. Tsunoda, J.F. Vickrey, L. Guerin, Sources of F region ionization enhancements in the nighttime auroral zone, J. Geophys. Res., 90(A8), 7533-7546, 1985.

Rottger , J., The macro-scale structure of equatorial spread-F irregularities, J. Atmos. and Terr. Phys., 38, 97-101, 1976.
Rottger, J., Wave-like structures of large-scale equatorial spread-F irregularities, J. Atmos. and Terr. Phys., 35, 1195-1206, 1973.
Singh, M., P. Rodriguez, and E.P. Szuszczewicz, Spectral classification of medium scale high latitude F region plasma density irregularities, J. Geophys. Res., 90 (A7), 6525-6532, 1985.
Spiro, R. W., R.A. Heelis, W.B. Hanson, Ion convection and the formation of the mid-latitude F region ionization trough, J. Geophys. Res., 83 (A9) 4255-4264, 1978.
Stein, S., Fading channel issues in system engineering, IEEE J. on Selected Areas in Communication, SAC-5 (2), 68-89,1987.
Szuszczewicz, E. P., M. Singh, and J.C. Holmes, Satellite and rocket observations of equatorial spread F irregularities: a two dimensional model, J. Atmos. Terr. Phys., 43,779, 1981.
Szuszczewicz, E. P., R.T Tsunoda, R. Narcisi, and J.C. Holmes, Coincident radar and rocket observations of equatorial spread F, Geophys. Res. Lett., 7, 537, 1980.
Szuszczewicz, E.P., Theoretical and experimental aspects of ionospheric structure: A global perspective on dynamics and irregularities, Radio Sci., 21(3), 351-362, 1986.
Tsunoda, R. T., High latitude F region irregularities: a review and synthesis, Revs. of Geophys., 26 (4), 719-760, 1988.
Wagner, L.S. and J.A. Goldstein, Response of the high latitude HF skywave channel to an isolated magnetic disturbance, Proc. of the fifth International Conference on HF radio systems and techniques, IEE, Edinburgh, 1991.
Wagner, L.S. J.A. Goldstein, M.A. Rupar, E.J. Kennedy, Northern Exposure 92: An investigation of transauroral HF radio skywave propagation, NRL report, in process of publication, 1993(b).
Wagner, L.S., J.A. Goldstein, M.A. Rupar, E.J. Kennedy, Measurements of delay and Doppler spread on a 1300 km trans-auroral channel, 7th Int'l. Ionospheric Effects Symposium, Alexandria, Va., May 1993(a).
Woodman, R.F. and C. LaHoz, Radar observations of F region equatorial irregularities, J. Geophys. Res., 81(31), 5447-5466, 1976.

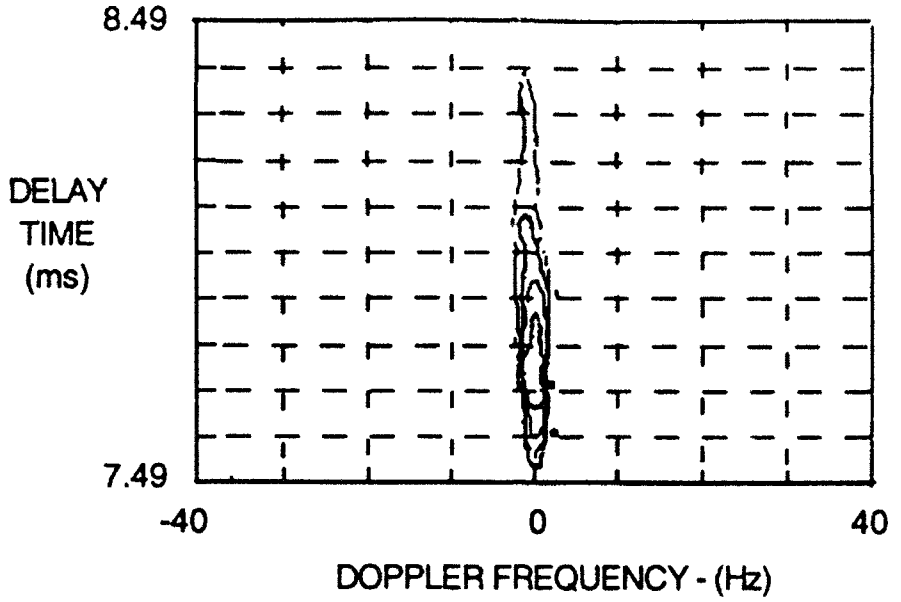

Fig. 1 - Scattering function for an east-west trans-equatorial path; 10.96 MHz; 1258 UT (2346 local meridian time); July 22, 1986; (adapted from Basler et al, 1987).

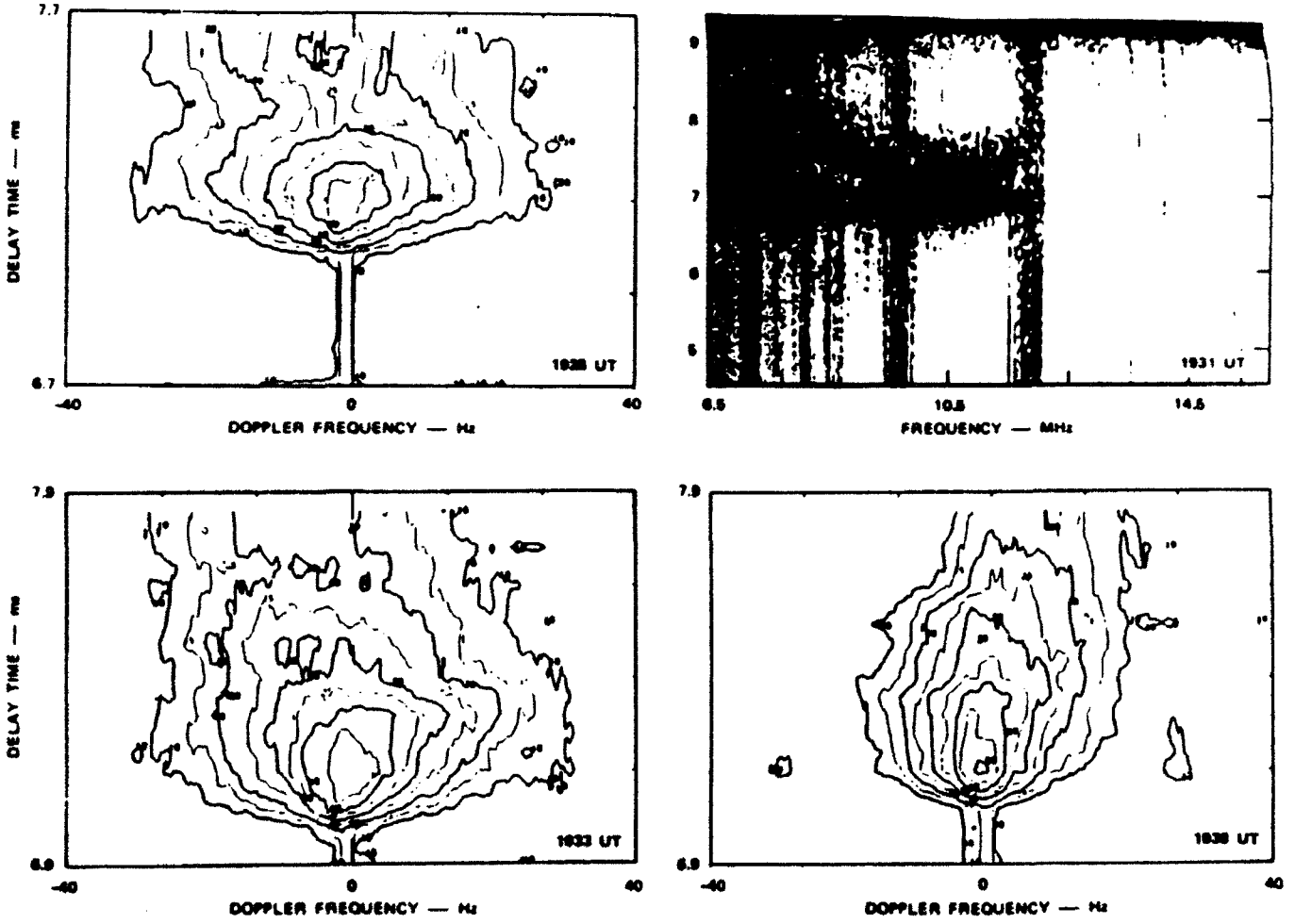

Fig. 2 - (a) Ionogram and scattering functions (10.75 MHz) for a north-south polar path; ~ 1930 UT, 3 October, 1984; [from Basler et al, 1987].

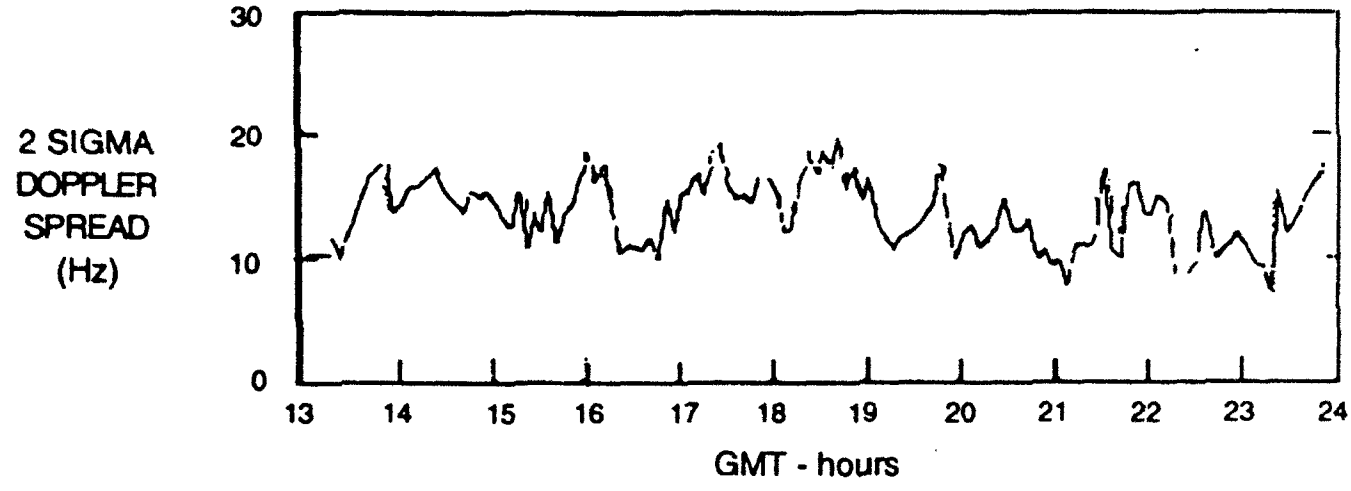

Fig. 3 - Mean 2σ Doppler spread values for the solar minimum, equinoctial periods October '84 and March '85; 9adapted from Basler et al, [1987]).

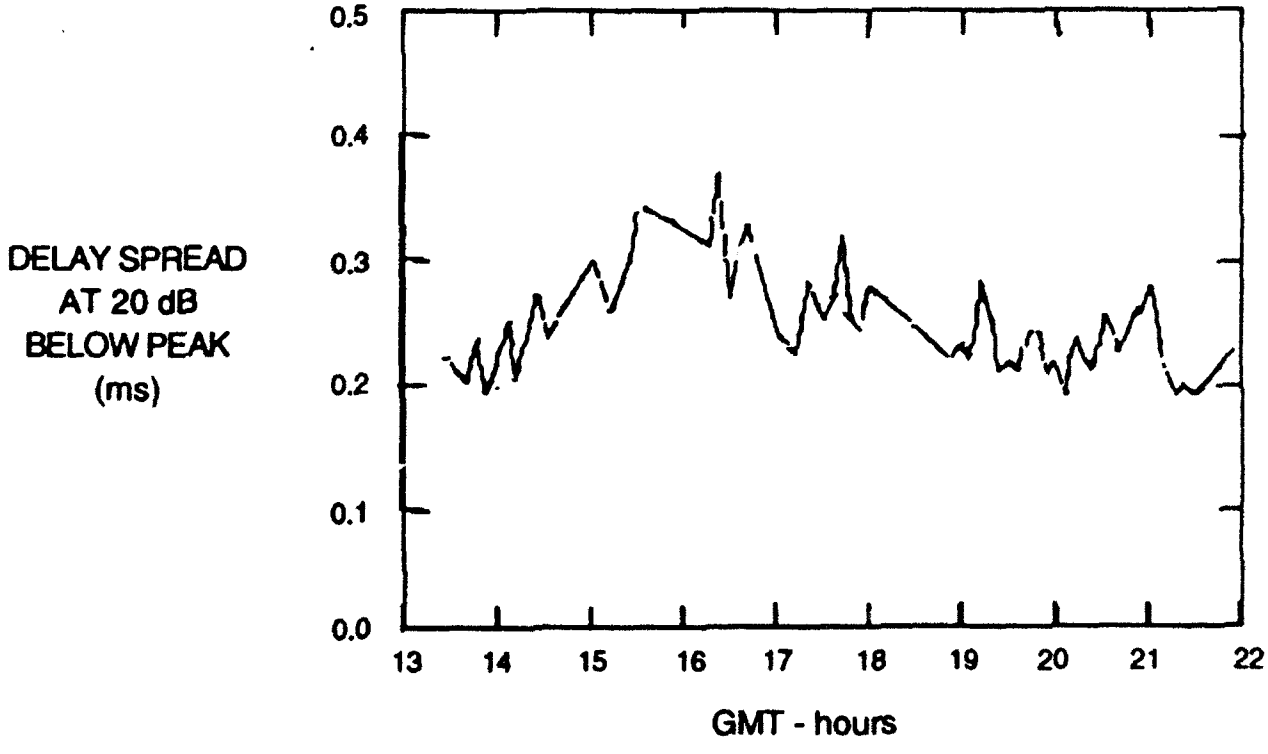

Fig. 4 - Mean delay spread for contours 20 dB below the signal peak for the solar minimum, equinoctial periods October '84 and March '85; (adapted from Basler et al, [1987]).

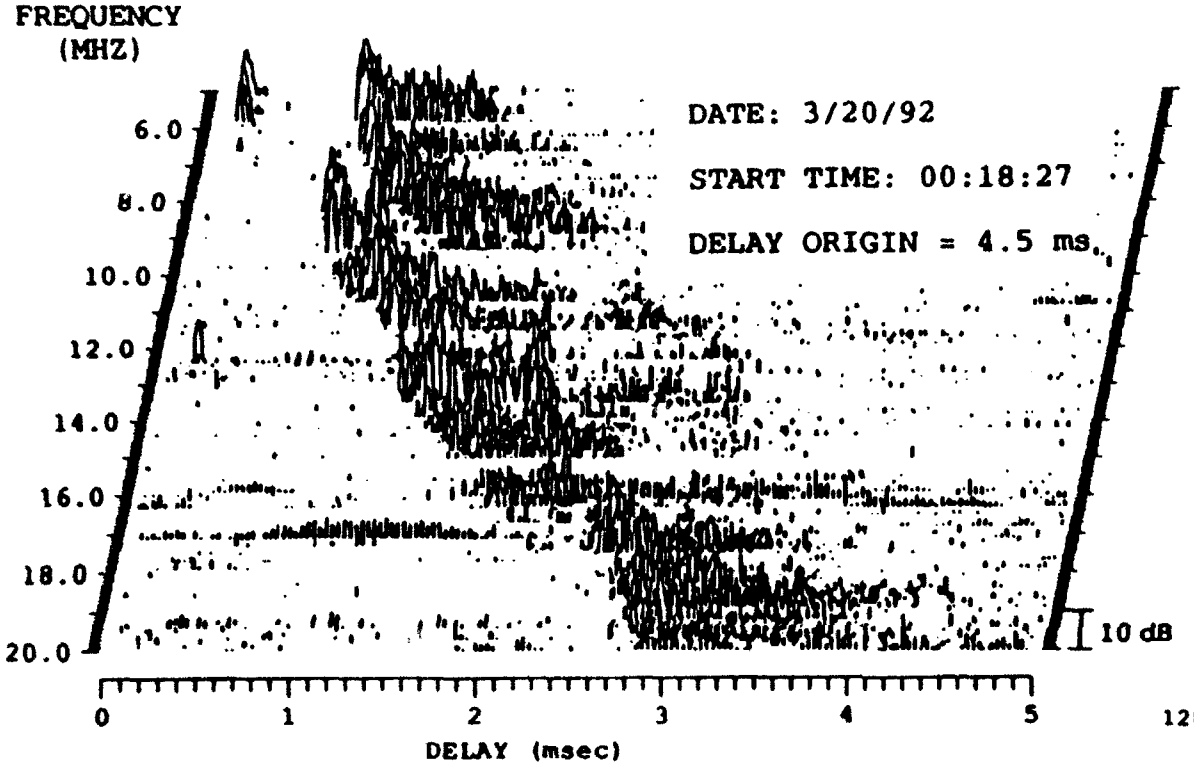

Fig. 5 - Midnight ionogram, Sondrestrom-Keflavik.

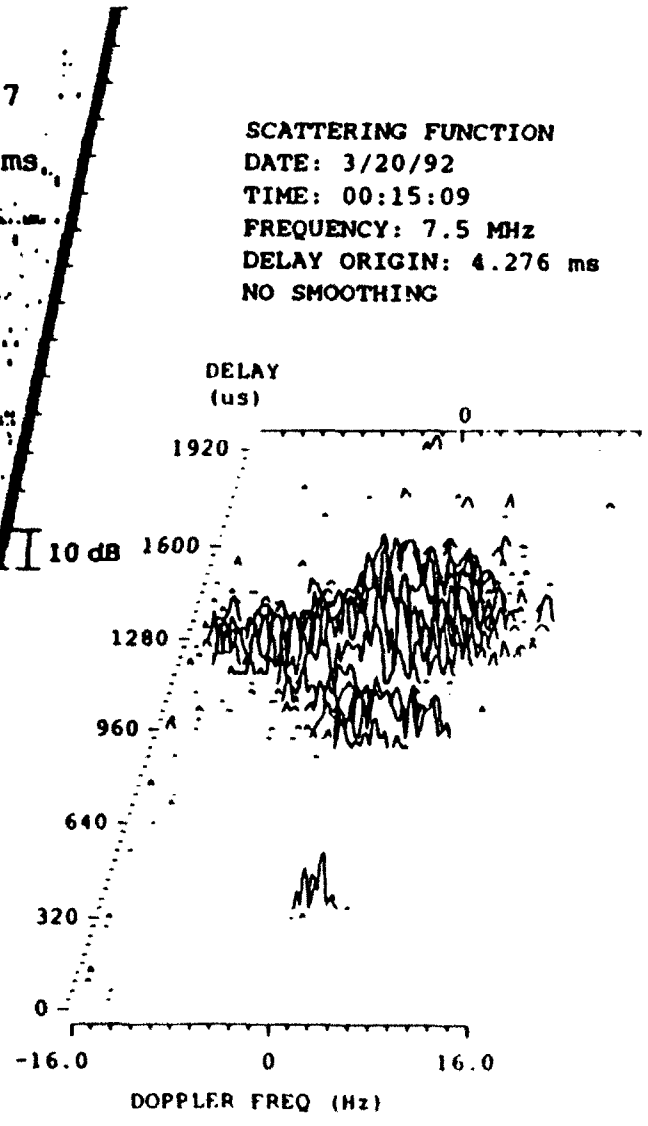

Fig. 6 - Scattering function (7.5 MHz), midnight trans-auroral path, Sondrestom-Keflavik.

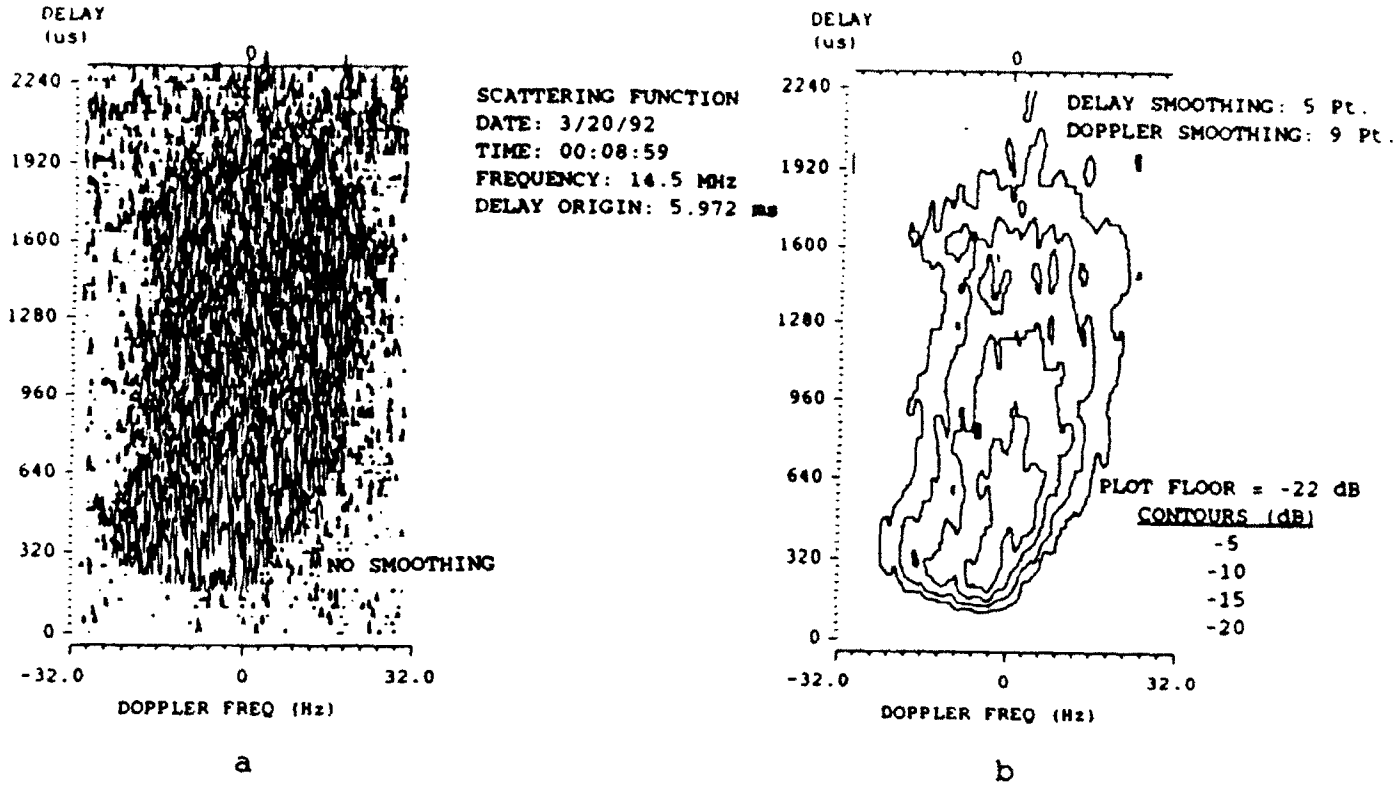

Fig. 7 - scattering function for midnight slant F scatter signal; trans-auroral channel; 14.5 MHz.

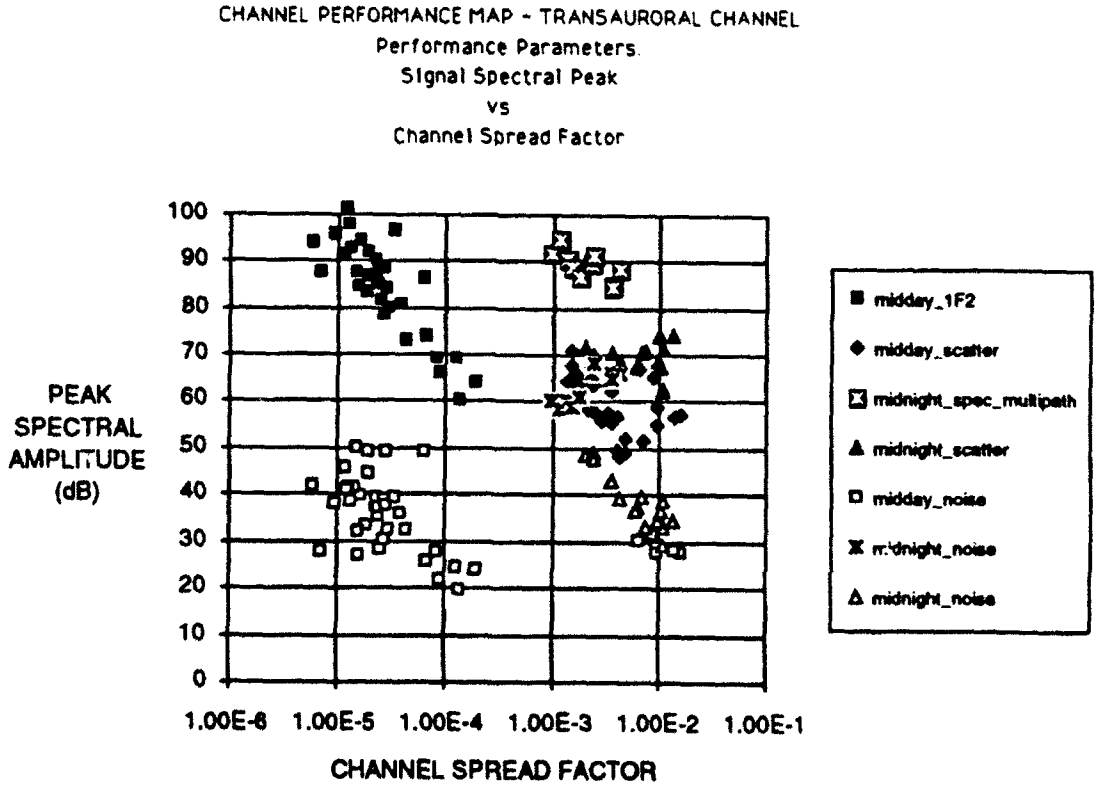

Fig. 8 - Channel performance map - trans-auroral channel; midday and midnight measurements.